ACS APPLIED MATERIALS & INTERFACES

Research Article

www.acsami.org

Antibacterial Adhesion of Borneol-Based Polymer via Surface Chiral Stereochemistry

Lingqiong Luo,[†] Guofeng Li,[†] Di Luan,[†] Qipeng Yuan,[†] Yen Wei,[‡] and Xing Wang*[,†]

[†]College of Life Science and Technology, Beijing University of Chemical Technology, Beijing 100029, P. R. China

[‡]Department of Chemistry and the Tsinghua Center for Frontier Polymer Research, Tsinghua University, Beijing 100084, P. R. China

Supporting Information

ABSTRACT: During its adhesion on external surfaces, a cell exhibits obvious inclination to different molecular chirality, which encourages us to develop a new type of antibacterial material catering to the "chiral taste" of bacteria. On the basis of the natural product borneol (a camphane-type bicyclic monoterpene), a series of borneol-based polymer, polyborneolacrylate (PBA), was successfully prepared and showed superior antibacterial adhesion properties resulting from the borneol isomers on material surface. The results of this study reveal that bacteria simply dislike this type of stubborn surface of PBA, and the PBA surface stereochemistry contributes to the interfacial antibacterial activities. The PBA polymers were evaluated as noncytotoxic and can be simply synthesized, demonstrating their great potential for biomedical applications.

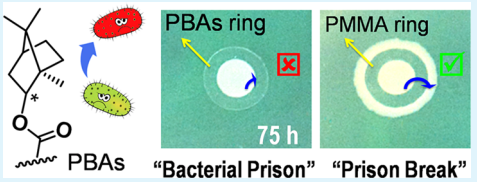

KEYWORDS: *antibacterial adhesion, biomaterial, borneol, chirality, stereochemistry, polymer*

1. INTRODUCTION

The prevention of bacterial adhesion on material surfaces is an important research topic,[1,2] as the adhesion of bacteria is the first step in bacterial colonization or proliferation as well as the formation of bacterial biofilms,[3] which are responsible for numerous human healthcare (i.e., infections and diseases) and environmental problems.[4] Various strategies have been explored mainly based on the immobilization or release of bactericidal substances[1−3,S−13] such as antibiotics,[7] metal derivatives,[8] graphene derivatives,[9] and poly(ammonium salts).[10] However, they are still not satisfactory because of their limited efficiency, the cytotoxicity, and the alarming case of antibiotic resistance, while antimicrobial peptides,[11] bacteriolytic enzymes,[12] and essential oils[13] are recognized as new and emerging natural strategies. These fascinating natural compositions were developed by nature over millions of years. Thus, living plants and animals have successfully constructed a complex defense system to cope with the ever-present threat of pathogens.[2] However, for biomedical applications, some tangible disadvantages cannot be ignored, such as biological stability and safety problems.[2] To date, few of those peptides or enzymes have proceeded into clinical trials.[14] Therefore, essential oils present more opportunities. They are known as a treasure house of diverse natural compounds and offer plentiful sources for the design of antibacterial materials. For example, Campo's group recently reported that polymer-bound Cl-catechols could effectively prevent biofilm formation.[15] However, from the inner mechanism, most existing antibacterial materials act predominantly by disrupting the integrity of cell membranes through interaction with the phospholipid component[16−18] or by influencing the bacterial functions through a poisoning model.[2] To date, utilizing the "senses" of bacterial cells on material surfaces to induce subsequent selective attachments or not, which is a new way to design biomedical materials and interfaces for antibacterial adhesion, is barely reported.

Focusing on the interactions at the interface between artificial materials and biological systems,[19−23] our previous work has demonstrated that a chiral biointerface can significantly influence cell adhesion and protein adsorption,[21,22] where hydrophobic interactions based on chiral stereochemistry are also an important factor.[23] However, for the wide array of pathogens, still less is known about aforementioned influencing factors. On the basis of the current understanding of chiral effects and hydrophobic interactions at biointerfaces, and inspired by the natural product borneol,[24,25] a chiral bicyclic monoterpene as shown in Scheme 1, we devoted attention to utilizing borneol to design a novel antibacterial material and develop an advanced strategy for antibacterial adhesion through polymer surface stereochemistry.

Borneol is a suitable model compound because of several outstanding properties. First, it is a known natural drug that is present in numerous medicinal plants, including *valerian*, *lavender*, *chamomile*, etc.[24] Borneol has four configurations that correspond to different positions of the hydroxyl group (three products, as shown in Scheme 1): *endo*-L-borneol, *endo*-D-borneol, and *exo*-isoborneol. They are ideal chiral units with a hydrophobic molecular structure. Second, borneol has various biomedical functions;[25,26] most importantly, it has been shown that esterification results in derivatives with increased activity compared to the parent borneol.[25] Thus, we deduce that borneol will not lose its activity after being grafted into a

Received: August 14, 2014
Accepted: October 21, 2014
Published: October 21, 2014

   dx.doi.org/10.1021/am505481q | ACS Appl. Mater. Interfaces 2014, 6, 19371−19377

Scheme 1. The Synthesis Processes of the Borneol-Based Polymers Polyborneolacrylates, Which Are Denoted as PLBA, PDBA, and PIBA According to the Three Chiral Borneol Monomers (LBA, DBA, and IBA) Used There[a]

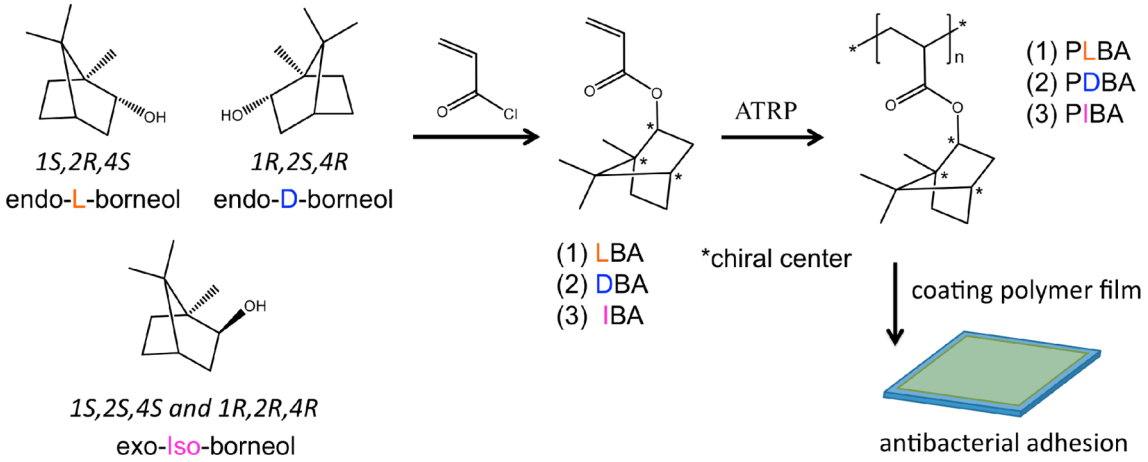

[a]The three kinds of parent borneol are *endo*-L-borneol, *endo*-D-borneol, and *exo*-isoborneol. They totally have four configurations including (1*S*,2*R*,4*S*), (1*R*,2*S*,4*R*), and (1*S*,2*S*,4*S*) and (1*R*,2*R*,4*R*).

polymer system. Moreover, the chiral feature or function will be largely enhanced by forming polymers.[22] For these reasons, borneol-based polymers will be effective for influencing bacterial senses and thus can be a new sort of surface for antibacterial adhesion.

2. EXPERIMENTAL SECTION

2.1. Monomer Synthesis. Borneol (1.00 g, 6.48 mmol) was first dissolved in 20 mL of tetrahydrofuran (THF). Triethylamine (0.98 g, 9.72 mmol) and acryloyl chloride (0.88 g, 9.72 mmol) were added into the above solution successively. Then, the reaction was allowed to proceed for 12 h with stirring at 35 °C. After filtration and rotary evaporation, a yellow-brown oil was obtained. Deionized water (20 mL) was added. The monomer was then extracted with ether (3 × 20 mL), and the organic phase was dried with anhydrous sodium sulfate. Finally, the target product, borneol acrylate (BA), was obtained by filtration, evaporation, and further purification by silica gel column chromatography (200−300 mesh, Sinopharm Chemical Reagent Co., Ltd., China; the eluents were petroleum ether/ethyl acetate = 4:1) with a yield > 95%.

2.2. Polymer Synthesis. Polymerization was achieved by adding ammonium persulfate (1.0 mg mL^{-1} of water solution, 10 μL) as an initiator into a degassed solution of methanol (200 μL) with the BA monomer described above (200 mg, 0.96 mmol) for 4 h at 70 °C. The polymer was purified by alternate treatments with dichloromethane (dissolution) and methanol (precipitate). The product was obtained as a white solid. With this method, the polymer molecular weights were approximately 10^5 g mol^{-1} with polydispersities of D = 3−5 (Supporting Information, Figure S4 and Table S1). These bulk polyborneolacrylate (PBA) polymers were used to coat polymer films (Supporting Information, Figure S5). Depending on the BA monomer used, the PBA was denoted as PLBA, PDBA, or PIBA (Scheme 1).

2.3. Antibacterial Adhesion Experiments. A "prison break" experiment was designed to evaluate the antibacterial adhesion capability of the PBAs. The PLBA, PDBA, PIBA, and the control poly(methyl methacrylate) (PMMA) films were cut into circular rings. The thickness of each ring is ∼10 μm. They are similar in weight, approximately 1.0 mg for PMMA and approximately 1.1 mg for PBAs. The rings were sterilized under ultraviolet light and fixed onto beef-protein medium, in which peptone (3 g), beef extract (5 g), NaCl (5 g), and agar (20 g) were dissolved in deionized water (1000 mL) at pH 7. After that, 1 μL of *Escherichia coli* (*E. coli*) suspension (10^6 CFU mL^{-1}) was added into the center of the circular ring and cultured at 37 °C. The results at different time points were recorded by camera. For this evaluation, each experiment was repeated at least five times.

The standard bacteria coincubation experiments were performed to study interactions between bacteria and the PBA surfaces. *E. coli* and *Staphylococcus aureus* (*S. aureus*) were used here. Sticker modules opened with a window section were fixed on the polymers (PLBA, PDBA, PIBA, and PMMA, Scheme S3 in Supporting Information). These modules were sterilized under ultraviolet light and then immersed in 120 mL of dilute bacteria suspension (*E. coli* or *S. aureus*), prepared freshly in normal saline (10^6 CFU mL^{-1}). After a specified period of incubation at 4 °C, the modules were removed and gently rinsed with phosphate buffer saline (PBS) three times. Then, the substrates were removed to obtain the polymer sections, which were used to evaluate bacterial attachment by optical microscopy. For this evaluation, each experiment was repeated at least five times.

Optical density (OD) testing and the plate count methods were also used to study aforementioned bacterial attachment. The sticker modules were immersed in 120 mL of dilute *E. coli* suspension for approximately 60 h. After rinsing gently with PBS three times, the polymer sections were incubated in fresh culture medium at 37 °C. *E. coli* outgrowth was estimated by monitoring the OD changes in each well at 600 nm every 3 h for a total of 24 h. In addition, after 9 h of culture, 10 μL of *E. coli* suspensions were taken out and serially diluted 7-fold. Then, 100 μL of the diluents were cultured on beef-protein medium and further cultured for 24 h at 37 °C. The numbers of *E. coli* colonies were counted.

2.4. MTT Assay. The biocompatibility of the materials was investigated with L929 fibroblast cells. Briefly, the PBA films (1.5 cm × 2 cm) were sterilized with ultraviolet light and immersed in 2 mL of 1640 medium for 24 h. The obtained conditioned solution was used as complete cell culture medium after adding 10% FBS, 100 units mL^{-1} penicillin, and 100 μg mL^{-1} streptomycin. L929 fibroblast cells (purchased from Cell Resource Center, IBMS, CAMS/PUMC, Beijing, China) were cultured in the conditioned medium at 37 °C in a humidified environment of 95% air and 5% CO_2. After 48 h of incubation, cell viability was determined by the 3-(4,5-dimethylthiazol-2-yl)-2,5-diphenyltetrazolium bromide (MTT) assay kit based on the manufacturer's instructions. The relative growth rate (RGR) of the cells was calculated according to the following formula: RGR (%) = $Abs_{490\ sample}/Abs_{490\ control}$ × 100. Finally, toxicity grades were assessed.

3. RESULTS AND DISCUSSIONS

3.1. Synthesis and Characterization of the Borneol-Based Polymers. The borneol-based polymers were designed as comb polymers of PBA (as shown in Scheme 1). Briefly, the BA monomers were first synthesized according to an acylation reaction, and then the PBAs were prepared via atom transfer

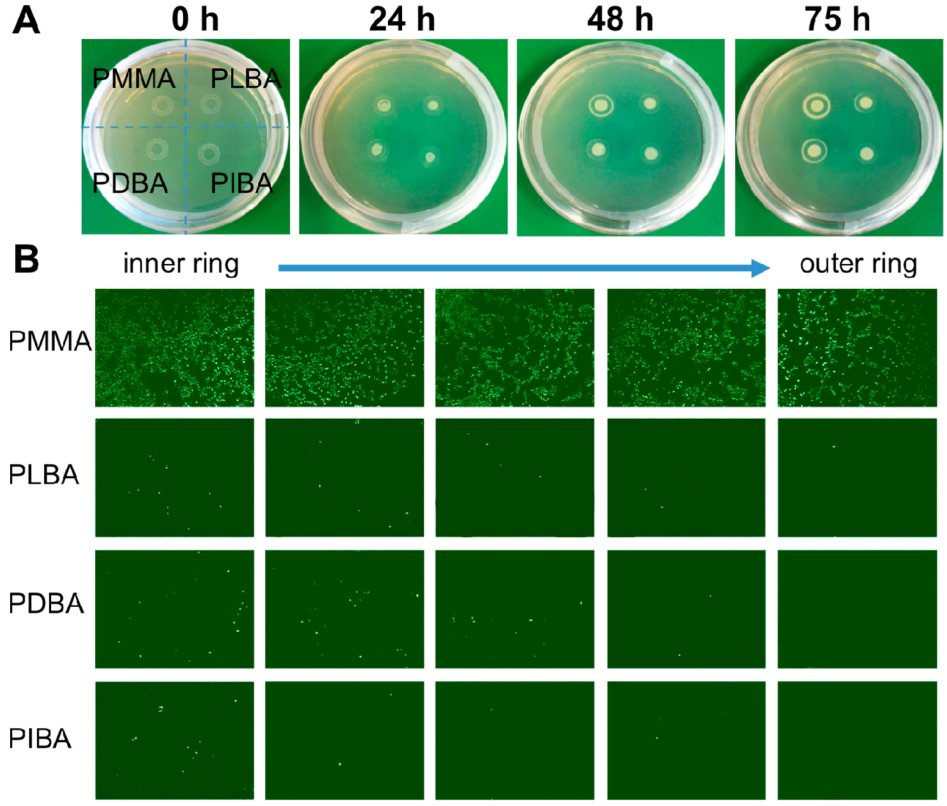

Figure 1. (A) Effects on controlling the escape of *E. coli* from PMMA, PLBA, PDBA, and PIBA rings after different periods of incubation time. (B) Optical micrographs of *E. coli* adhered on the above polymers from the inner (left) to outer (right) edges of the rings after 60 h of incubation. The image size is approximately 897 μm^2 (34.5 $\mu m \times 26.0$ μm).

radical polymerization (ATRP).[21,22] Figure S3 in Supporting Information shows the circular dichroism (CD) spectra of the different monomers and polymers at the same effective concentration. The spectra show strong mirror-image responses in the region of 210−250 nm, reflecting the intrinsic chirality of PLBA and PDBA (Supporting Information, Figure S3B). In contrast, PIBA gave almost no CD signal at approximately 230 nm, because it consists of a racemic mixture. This study showed that optical rotation was largely amplified after polymerization compared to the original monomer state (Supporting Information, Figure S3A). This CD detection also verified that the synthesis processes maintained the molecular chirality.

3.2. Antibacterial Adhesion Capability. To demonstrate the antibacterial activity of PBAs, a bacterial "prison break" experiment was designed to evaluate the antibacterial adhesion capability of the PBAs. Briefly, PLBA, PDBA, PIBA, and PMMA films (Supporting Information, Figure S5; the thickness was approximately 10 μm in the dry state; PMMA was used as control because of its simple stereochemistry) were cut into circular rings (the inner diameter was 6 mm, the outer diameter was 10 mm), sterilized under ultraviolet light, and fixed onto beef-protein medium (Figure 1A). Next, 1 μL of *E. coli* suspension (10^6 CFU mL^{-1}) was added into the center of the circular ring and cultured at 37 °C. The growth of the *E. coli* after different periods of time was observed and recorded with a camera. For this evaluation, each experiment was repeated at least five times.

Naturally, we observed the expanding growth of *E. coli* in the polymer rings as shown in Figure 1A. In the first 12 h, a clear-cut *E. coli* stain was formed, but none of the stain touched the edges of the polymer rings. After 24 h, *E. coli* covered almost the entire inner ring sections. At this time point, the PMMA ring had failed to act as a "prison" to control the escape of bacteria. Rather, *E. coli* colonies were able to move beyond the PMMA ring, resulting in a white surrounding outside. However, the PBA rings exhibited good control. No *E. coli* colonies had escaped the PBA "prison" after 48 h of incubation, whereas the white *E. coli* colonies had expanded out of the PMMA ring and occupied a much larger region. This experiment was performed more than five times (see Supporting Information, Figure S8A−E). To our surprise, in some instances the resistance capability could be maintained for more than 100 h on a given single PBA ring. Deeper investigations were carried out by photomicrography (the samples were taken from the experiment after 60 h of incubation as shown in Supporting Information, Figure S8E). We scanned the polymer rings from their inner to outer edges, and the results are shown in Figure 1B. *E. coli* cells were spread over almost the entire surface of PMMA, as a higher but similar cell density was observed. However, there was a low density of bacterial cells only at the inner ring of the PBAs, and few cells appeared at outer ring of all the PBAs. This result confirmed the antibacterial adhesion capability of PBAs. In addition, polymer rings with different width were utilized to evaluate this effect. The results (see Supporting Information, Figure S9) showed that the wider PMMA still could not block the escape of *E. coli*, while PIBA could act as a prison in the same incubation time. Therefore, the antibacterial capability of PBA rings was caused by a biological surface recognizing rather than a physical effect of blocking.

The standard bacteria coincubation experiments were also performed to further study interactions between bacteria and

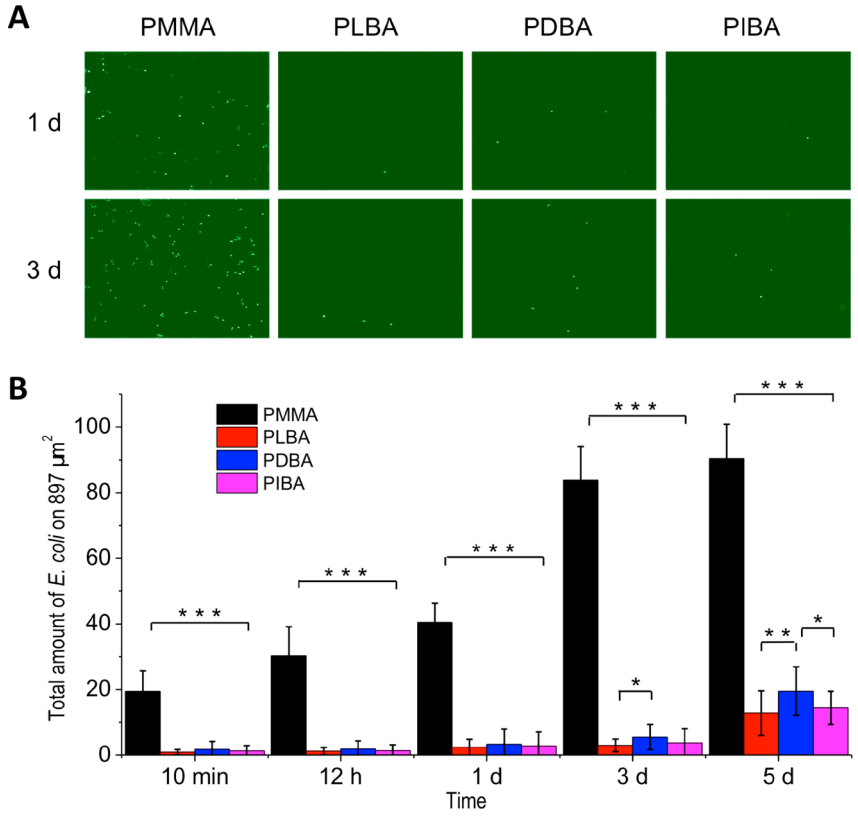

Figure 2. (A) Optical micrographs of *E. coli* adhered on PMMA, PLBA, PDBA, and PIBA films for different periods of time. The image size is approximately 897 μm^2 (34.5 μm × 26.0 μm). (B) Quantitative data for *E. coli* attachment on the polymer films at the corresponding time points. The results were obtained from five independent experiments. Significant differences: *: $P < 0.05$; **: $P < 0.01$; ***: $P < 0.001$.

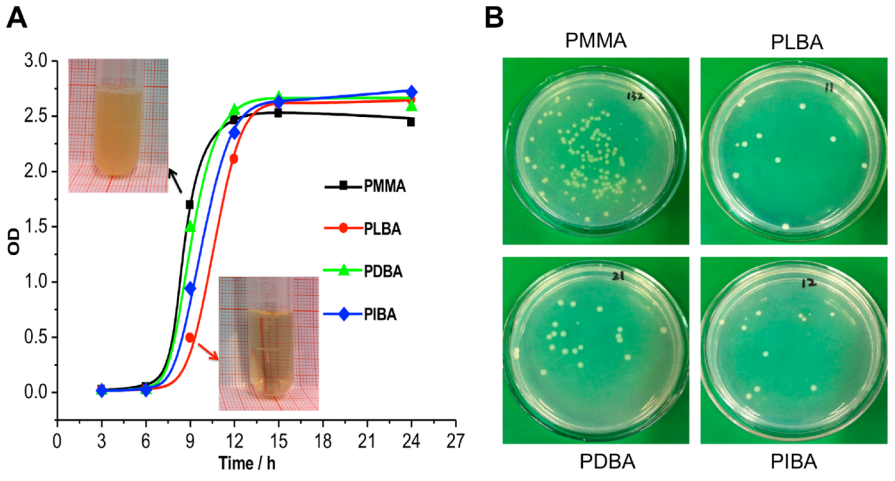

Figure 3. (A) Optical density (OD_{600}) test to evaluate the PBA and PMMA films, which were soaked in an *E. coli* suspension for 60 h and then transferred to fresh culture medium for the OD_{600} testing. (B) The *E. coli* colony numbers are from plate count experiments. The colony numbers corresponding to viable *E. coli* on PMMA, PLBA, PDBA, and PIBA films were 132, 11, 21, and 12 units, respectively.

the PBA surfaces. Figure 2A shows typical microscopic images after different periods of time for the *E. coli* attachment assay on films of PMMA, PLBA, PDBA, and PIBA (see Supporting Information, Figure S10 for all the specified time points). In particular, after 1 d of incubation, a clear distribution of *E. coli* cells was observed. But, barely a few *E. coli* cells could be found on the PBA surfaces. In fact, only after 10 min of incubation, a small amount of *E. coli* had attached onto the PMMA film (Supporting Information, Figure S10). At longer incubation times (Figure 2A, 3 d), increased amounts of *E. coli* adhered onto the PMMA surface. However, for the PBA surfaces, even after 3 d of incubation, only a few of *E. coli* cells were found on the films, indicating strong suppression of *E. coli* adhesion. These distinct phenomena were mainly related to the polymer surface stereochemistry of borneol, as statistical analysis of the quantitative data (Figure 2B) indicated very significant difference between PMMA and the PBAs (*t* test: $P \ll 0.001$) at all time points. The surface chirality of the PBA polymers might also contribute to some of the antibacterial efficiency, and statistical analysis showed some significance among the

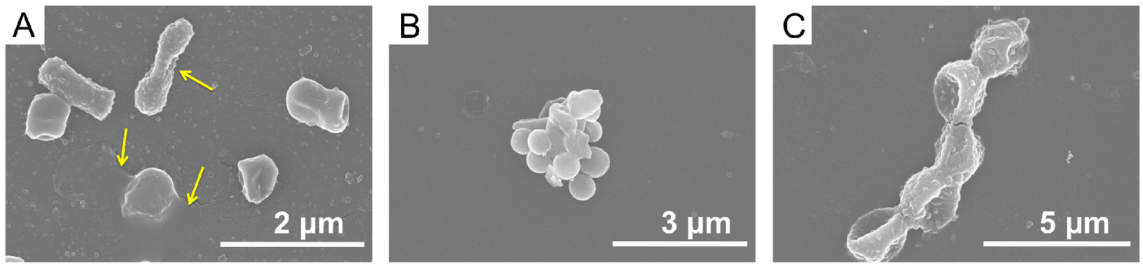

Figure 4. SEM images of cells cultured on PLBA film. (A) *E. coli*, (B) *S. aureus*, and (C) *M. racemosus* after incubation for 3 d at 37 °C.

chiral PBA films after the 3 d time point. Specifically, PLBA displayed more resistance to *E. coli* cells than PIBA and PDBA. However, significance was only found between PLBA and PDBA (t test: $P < 0.05$). No significant differences were found between PLBA and PIBA, or between PIBA and PDBA. After 5 d, the difference became more significant between PLBA and PDBA (t test: $P < 0.01$). While significance was found between PIBA and PDBA (t test: $P < 0.05$), no distinct difference was found between PLBA and PIBA. These phenomena indicated that the PLBA and PIBA films possess better antibacterial activity than the PDBA film.

To demonstrate the above-mentioned bacterial behavior, classical methods such as the optical density (OD) test and plate count method were employed. Figure 3A shows the OD test results for the four types of polymer films, which were soaked in an *E. coli* suspension for over 60 h and were subsequently transferred and incubated in fresh culture medium. For the first 6 h, *E. coli* were in a lag phase and were adapting to the new environment, except for the *E. coli* on PMMA that took the lead in moving into the logarithmic phase. Distinct differences were found among the four test groups after 9 h of incubation, as the OD values displayed a clear gradation of bacterial densities from low to high in the order of PLBA, PIBA, PDBA, and PMMA (also see Supporting Information, Figure S12). The upward trends for the PBAs continued until 15 h, when the *E. coli* entered into the stationary phase. These results suggest that PLBA may have the best efficiency in terms of *E. coli* inhibition. Furthermore, the *E. coli* colony numbers from the plate count experiments verified the above effect (see Experimental Section for the experimental details). As shown in Figure 3B, the number of viable *E. coli* colonies on PMMA (132 units) was obviously 10 times higher compared to that on the PLBA (11 units) and PIBA (12 units) films. Although no difference was found between the PLBA and PIBA films, the PDBA film exhibited weaker antibacterial properties because 21 units were counted on the plate in this test. Regardless, the regulation is very consistent with our primary findings.

3.3. Broad-Spectrum Antimicrobial Activity. Subsequently, we performed antibacterial experiments with *S. aureus*, a typical Gram-positive bacterium. The PBAs showed a similar resistance gradient for *S. aureus* adhesion when evaluated after 4 d (see Supporting Information, Figure S11A). However, no statistical significance was found among the borneol chiral configurations of PBAs (Supporting Information, Figure S11B), perhaps due to the relatively slower proliferation rate of *S. aureus*. Scanning electron microscopy (SEM) characterization also showed distinct surface antiadhesion for *E. coli*, *S. aureus*, and furthermore for *Mucor racemosus* (*M. racemosus*, typical fungi) cells on the PBAs (see Supporting Information, Figure S13 for all details). Additional studies with SEM revealed that the bacterial morphologies became shriveled to a certain degree on the PBA films (typical images are shown in Figure 4). Furthermore, in some cases, the bacteria lost their cellular integrity after being exposed to PBA films (Figure 4A). This result highlights that irreversible damage can be induced on bacterial cells once they make direct contact with PBA films, although the major event is antiadhesion.

3.4. Study on the Mechanism. The differential behavior of bacteria toward the polymer surfaces not only demonstrated superantibacterial capability of the PBA polymers but also suggested that bacteria perceive the different signals related to the surface stereochemistry of the polymer. From the microscale of the molecular structures, the methyl comb-teeth of PMMA are simple compared to the PBAs that possess dense pendants of camphane-type bicyclic structures, which have complex carbon stereochemistry. It has been reported that polymers such as polyethylene, polystyrene, and linear aliphatic polyacrylates are less effective for antibacterial adhesion,[27,28] perhaps due to their simple stereochemistry. However, the camphane-type bicyclic structure of borneol has three chiral centers, located at C^1, C^2, and C^4, as shown in Scheme 1, and those polymers exhibited excellent antibacterial capability. In particular, differences in antibacterial adhesion were found between PLBA/PIBA and PDBA (Figure 2B), where the D-configuration of borneol on the PDBA surface resulted in relatively weak antibacterial adhesion properties.

This regulation seems to disagree with previous studies on the topic of chiral biointerfaces,[21−23,29] where D surfaces tend to resist cell adhesion or protein adsorption. Although this paradox exists here, further consideration of the chiral borneol molecule indicated that the chiral configuration at C^2 is consistent with previous studies. For example, in PLBA (1*S*,2*R*,4*S*-borneol pendants), the C^2 chiral center corresponds to a D-configuration, which usually provides surfaces with antiadhesion properties for cells or proteins. Thus, we envision that bacteria may mainly distinguish the chiral center at C^2, rather than C^1 or C^4. In other words, the $O-C^2HR_1R_2$ stereochemistry may be the key point at which bacteria "sense" the chiral difference. Compared with the pendant $O-CH_3$ groups of the PMMA control, the bicyclic stereochemistry structure of borneol contributed greatly to antibacterial adhesion, because single $-CH_3$ stereochemistry could not prevent bacterial invasion. Thus, the above experiments revealed that carbon stereochemistry in a bicyclic structure is of great significance for antibacterial adhesion, and surface chirality contributes partly to the antibacterial efficiency.

Another question is that the PBA polymers have higher hydrophobicity. Water contact angle (CA) measurements (see Supporting Information, Figure S6) showed that the CA was 102 ± 2° on the PBAs, compared to 79 ± 1° on PMMA. However, in our viewpoint, hydrophobicity is not important for

this antibacterial activity. It is well-reported that the bacterial adhesion should be higher on hydrophobic than on hydrophilic surfaces.[27,30] In fact, no distinct regulation is found between wettability and antibacterial activity for the diverse materials.[31] Therefore, hydrophobicity did not play a crucial role on this antibacterial activity. Rather, we deduced that the key point is surface stereochemistry, and especially the bicyclic structure, which is crucial for PBAs antibacterial adhesion.

3.5. Biocompatibility Evaluation. A standard MTT assay showed that the PBA materials were noncytotoxic (the impregnating solutions were used in this assay). As shown in Figure 5, the RGR on PLBA and PDBA films was somewhat

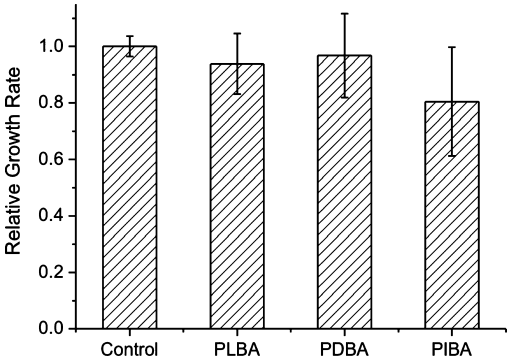

Figure 5. MTT results on RGR of L929 cells for 2 d of incubation in PBA conditioned media. The data are presented as the mean plus or minus the standard deviation (n = 10 for each group).

higher than that on the PIBA film, although the difference was not significant. The results shown in Table 1 demonstrated that

Table 1. MTT Test Results for the PLBA, PDBA, and PIBA Films

sample	days of culture	relative growth rate (%)	toxicity grade
PLBA	2	93.87 ± 10.69	1
PDBA	2	96.76 ± 14.85	1
PIBA	2	80.44 ± 19.22	1

the cell toxicity of the PBA films was in grade 1. According to the standard toxicity rating, grade 1 indicates no toxicity in the framework of safety for use. Different from a drug-release model, PBAs mainly prevent bacterial adhesion through stereochemical structures of the covalently bonded borneol units on the polymer surface. Cell culture experiments showed that the cells also did not prefer to adhere to the PBA surfaces (Supporting Information, Figure S14). From a biological point of view, bacteria simply dislike this type of stubborn surface. This stereochemistry mechanism, especially on PBA surfaces, has demonstrated the capability to resist colonization by diverse bacteria. In those conditions, borneol molecules or borneol derivatives do not act as bactericide in drug-release manner. However, if degradation occurs in the long run (Supporting Information, Figure S7 evaluated the degradation of PBAs *in vitro*), the catabolin should also be of benefit for antibacterial activity. At least, the mice subcutaneous tissue implant of PLBA film did not generate any inflammatory response to the surrounding tissue cells. Work investigating above possibility is currently underway.

4. CONCLUSION

In conclusion, we have developed novel PBA polymers as antibacterial materials or coatings. PLBA displayed the best performance due to its outstanding antibacterial activity and good biocompatibility. An additional thought on this natural strategy is that borneol is a chiral drug. To date no drug-resistance is reported maybe because chiral stereochemistry has a unique meaning for life. Thus, these biocompatible polyborneol PBAs might be persistently effective for antibacterial applications. Importantly, the proof-of-concept demonstration in our study showed that utilizing polymer surface stereochemistry is an advanced strategy for antibacterial adhesion. The insights gained regarding the effects of surface stereochemistry and chiral differences may help us to tailor the antibacterial performance of a new generation of polymer films. Ultimately, this work will advance both the research and application of antibacterial materials in the field of biomedicine.

■ ASSOCIATED CONTENT

Ⓢ Supporting Information

Synthesis route and CD, NMR, GC-MS, and GPC characterizations; film coating and water contact angle measurements; optical micrographs and SEM images of the antibacterial experiments. This material is available free of charge via the Internet at http://pubs.acs.org.

■ AUTHOR INFORMATION

Corresponding Author

*E-mail: wangxing@mail.buct.edu.cn.

Notes

The authors declare no competing financial interest.

■ ACKNOWLEDGMENTS

The authors thank the National Natural Science Foundation of China (21204004), the Beijing Natural Science Foundation (2132040), and the Specialized Research Fund for the Doctoral Program of Higher Education (20120010120011) for their funding support. Helpful discussions with Prof. L. Tao, of the Dept. of Chemistry, Tsinghua University, are greatly appreciated.

■ REFERENCES

(1) Banerjee, I.; Pangule, R. C.; Kane, R. S. Antifouling Coatings: Recent Developments in the Design of Surfaces That Prevent Fouling by Proteins, Bacteria, and Marine Organisms. *Adv. Mater.* **2011**, *23*, 690−718.

(2) Glinel, K.; Thebault, P.; Humblot, V.; Pradier, C. M.; Jouenne, T. Antibacterial Surfaces Developed from Bio-Inspired Approaches. *Acta Biomater.* **2012**, *8*, 1670−1684.

(3) Renner, L. D.; Weibel, D. B. Physicochemical Regulation of Biofilm Formation. *MRS Bull.* **2011**, *36*, 347−355.

(4) Wong, G. C. L.; O'Toole, G. A. All Together Now: Integrating Biofilm Research Across Disciplines. *MRS Bull.* **2011**, *36*, 339−342.

(5) Neu, T. R. Significance of Bacterial Surface-Active Compounds in Interaction of Bacteria with Interfaces. *Microbiol. Rev.* **1996**, *60*, 151−166.

(6) Lejars, M.; Margaillan, A.; Bressy, C. Fouling Release Coatings: A Nontoxic Alternative to Biocidal Antifouling Coatings. *Chem. Rev.* **2012**, *112*, 4347−4390.

(7) Hetrick, E. M.; Schoenfisch, M. H. Reducing Implant-Related Infections: Active Release Strategies. *Chem. Soc. Rev.* **2006**, *35*, 780−789.

(8) Rai, M.; Yadav, A.; Gade, A. Silver Nanoparticles as a New Generation of Antimicrobials. *Biotechnol. Adv.* **2009**, *27*, 76−83.

(9) Tu, Y. S.; Lv, M.; Xiu, P.; Huynh, T.; Zhang, M.; Castelli, M.; Liu, Z. R.; Huang, Q.; Fan, C. H.; Fang, H. P.; Zhou, R. H. Destructive Extraction of Phospholipids from *Escherichia Coli* Membranes by Graphene Nanosheets. *Nat. Nanotechnol.* **2013**, *8*, 594−601.
(10) Zhou, H.; Weir, M. D.; Antonucci, J. M.; Schumacher, G. E.; Zhou, X. D.; Xu, H. H. Evaluation of Three-Dimensional Biofilms on Antibacterial Bonding Agents Containing Novel Guaternary Ammonium Methacrylates. *Int. J. Oral Sci.* **2014**, 1−10.
(11) Haug, B. E.; Strom, M. B.; Svendsen, J. S. M. The Medicinal Chemistry of Short Lactoferricin-Based Antibacterial Peptides. *Curr. Med. Chem.* **2007**, *14*, 1−18.
(12) Kristensen, J. B.; Meyer, R. L.; Laursen, B. S.; Shipovskov, S.; Besenbacher, F.; Poulsen, C. H. Antifouling Enzymes and the Biochemistry of Marine Settlement. *Biotechnol. Adv.* **2008**, *26*, 471−481.
(13) Wang, L.; Liu, F.; Jiang, Y.; Chai, Z.; Li, P.; Cheng, Y.; Jing, H.; Leng, X. Synergistic Antimicrobial Activities of Natural Essential Oils with Chitosan Films. *J. Agric. Food Chem.* **2011**, *59*, 12411−12419.
(14) Guaní-Guerra, E.; Santos-Mendoza, T.; Lugo-Reyes, S. O.; Terán, L. M. Antimicrobial Peptides: General Overview and Clinical Implications in Human Health and Disease. *Clin. Immunol.* **2010**, *135*, 1−11.
(15) García-Fernández, L.; Cui, J.; Serrano, C.; Shafiq, Z.; Gropeanu, R. A.; San Miguel, V.; Ramos, J. I.; Wang, M.; Auernhammer, G. K.; Ritz, S.; Golriz, A. A.; Berger, R.; Wagner, M.; del Campo, A. Antibacterial Strategies from the Sea: Polymer-Bound Cl-Catechols for Prevention of Biofilm Formation. *Adv. Mater.* **2013**, *25*, 529−533.
(16) Salditt, T.; Li, C.; Spaar, A. Structure of Antimicrobial Peptides and Lipid Membranes Probed by Interface-Sensitive X-ray Scattering. *Biochim. Biophys. Acta* **2006**, *1758*, 1483−1498.
(17) Kalemba, D.; Kunicka, A. Antibacterial and Antifungal Properties of Essential Oils. *Curr. Med. Chem.* **2003**, *10*, 813−829.
(18) Ait-Ouazzou, A.; Cherrat, L.; Espina, L.; Lorán, S.; Rota, C.; Pagán, R. The Antimicrobial Activity of Hydrophobic Essential Oil Constituents Acting Alone or in Combined Processes of Food Preservation. *Innovative Food Sci. Emerging Technol.* **2011**, *12*, 320−329.
(19) Hanein, D.; Geiger, B.; Addadi, L. Differential Adhesion of Cells to Enantiomorphous Crystal Surfaces. *Science* **1994**, *263*, 1413−1416.
(20) Sun, T. L.; Qing, G. Y.; Su, B. L.; Jiang, L. Functional Biointerface Materials Inspired from Nature. *Chem. Soc. Rev.* **2011**, *40*, 2909−2921.
(21) Wang, X.; Gan, H.; Sun, T. L.; Su, B. L.; Fuchs, H.; Vestweber, D.; Butz, S. Stereochemistry Triggered Differential Cell Behaviours on Chiral Polymer Surfaces. *Soft Matter* **2010**, *6*, 3851−3855.
(22) Wang, X.; Gan, H.; Sun, T. L. Chiral Design for Polymeric Biointerface: The Influence of Surface Chirality on Protein Adsorption. *Adv. Funct. Mater.* **2011**, *21*, 3276−3281.
(23) Wang, X.; Gan, H.; Zhang, M. X.; Sun, T. L. Modulating Cell Behaviors on Chiral Polymer Brush Films with Different Hydrophobic Side Groups. *Langmuir* **2012**, *28*, 2791−2798.
(24) Granger, R. E.; Campbell, E. L.; Johnston, G. A. R. (+)- And (−)-Borneol: Efficacious Positive Modulators of GABA Action at Human Recombinant $\alpha_1\beta_2\gamma_{2L}$GABA$_A$ Receptors. *Biochem. Pharmacol.* **2005**, *69*, 1101−1111.
(25) Dorman, H. J. D.; Deans, S. G. Antimicrobial Agents from Plants: Antibacterial Activity of Plant Volatile Oils. *J. Appl. Microbiol.* **2000**, *88*, 308−316.
(26) Mai, L. M.; Lin, C. Y.; Chen, C. Y.; Tsai, Y. C. Synergistic Effect of Bismuth Subgallate and Borneol, the Major Components of Sulbogin®, on the Healing of Skin Wound. *Biomaterials* **2003**, *24*, 3005−3012.
(27) Speranza, G.; Gottardi, G.; Pederzolli, C.; Lunelli, L.; Canteri, R.; Pasquardini, L.; Carli, E.; Lui, A.; Maniglio, D.; Brugnara, M.; Anderle, M. Role of Chemical Interactions in Bacterial Adhesion to Polymer Surfaces. *Biomaterials* **2004**, *25*, 2029−2037.
(28) Hook, A. L.; Chang, C. Y.; Yang, J.; Luckett, J.; Cockayne, A.; Atkinson, S.; Mei, Y.; Bayston, R.; Irvine, D. J.; Langer, R.; Anderson, D. G.; Williams, P.; Davies, M. C.; Alexander, M. R. Combinatorial Discovery of Polymers Resistant to Bacterial Attachment. *Nat. Biotechnol.* **2012**, *30*, 868−875.
(29) El-Gindi, J.; Benson, K.; De Cola, L.; Galla, H. J.; Seda Kehr, N. Cell Adhesion Behavior on Enantiomerically Functionalized Zeolite L Monolayers. *Angew. Chem., Int. Ed.* **2012**, *51*, 3716−3720.
(30) Bruinsma, G. M.; Van der Mei, H. C.; Busscher, H. J. Bacterial Adhesion to Surface Hydrophilic and Hydrophobic Contact Lenses. *Biomaterials* **2001**, *22*, 3217−3224.
(31) Hu, W. B.; Peng, C.; Luo, W. J.; Lv, M.; Li, X. M.; Li, D. Graphene-Based Antibacterial Paper. *ACS Nano* **2010**, *4*, 4317−4323.